

# Syntheses and X-ray Powder Structures of $K_2(ZrSi_3O_9) \cdot H_2O$ and Its Ion-Exchanged Phases with Na and Cs

Damodara M. Poojary, Anatoly I. Bortun, Lyudmila N. Bortun, and Abraham Clearfield\*

Department of Chemistry, Texas A&M University, College Station, Texas 77843

Received January 16, 1997<sup>®</sup>

A zirconium trisilicate compound, with composition  $K_2ZrSi_3O_9 \cdot H_2O$  (**1**), was prepared under mild hydrothermal conditions and was structurally characterized by using its X-ray powder diffraction data. The compound crystallizes in the space group  $P2_12_12_1$  with  $a = 10.2977(2)$  Å,  $b = 13.3207(3)$  Å,  $c = 7.1956(1)$  Å, and  $Z = 4$ . The asymmetric unit consists of a metal atom, a trisilicate group, and three lattice positions corresponding to two cations and a water oxygen atom. In the structure, the Zr atom is octahedrally coordinated by the six terminal oxygens of the trisilicate group. The trisilicate groups exist as linear chain polymers connected to each other through the Zr atoms. This arrangement leads to channels and cavities in the structure that are occupied by the cations and water molecules. The  $K^+$  ions in compound **1** were exchanged for  $Cs^+$  ions in two steps. In the first case about 50% of the  $K^+$  ions were exchanged to give a compound with composition  $K_{0.9}Cs_{1.1}ZrSi_3O_9 \cdot H_2O$  (**2**). Compound **2** was then loaded with additional  $Cs^+$  ions which resulted in a phase  $K_{0.5}Cs_{1.5}ZrSi_3O_9 \cdot H_2O$  (**3**). These exchanged phases retain the crystal symmetry of compound **1**, but their unit cell dimensions have expanded as a result of large  $Cs^+$  ions replacing the smaller  $K^+$  ions. Structure analyses of the exchanged phases show that the cations found in the cavities of compound **1** are highly selective for  $Cs^+$  ions. A small amount of Cs ions also go to a site in the large channel that is very close to that occupied by the water oxygen in compound **1**. In the absence of Cs, this site is filled with water molecules. The second cation found in the channel of **1** is partially occupied by water and  $K^+$  ions. The  $K^+$  ions in compound **1** were completely exchanged for  $Na^+$  ions, and the compound thus obtained,  $Na_2ZrSi_3O_9 \cdot H_2O$  (**4**), was treated with  $Cs^+$  ions in a manner similar to that carried out for compound **1**. The low  $Cs^+$  ion phase,  $Na_{0.98}Cs_{1.02}ZrSi_3O_9 \cdot H_2O$  (**5**), and the high  $Cs^+$  ion phase,  $Na_{0.6}Cs_{1.4}ZrSi_3O_9 \cdot H_2O$  (**6**), show ion distributions very similar to compounds **2** and **3** except for the fact that in the Na phases a small amount  $Cs^+$  ion also goes to the second cation site. Compound **1** on heating releases the lattice water and transforms into a hexagonal phase,  $K_2ZrSi_3O_9$ , corresponding to the mineral wadeite. In the high-temperature phase the silicate group exists as a condensed cyclic group and the  $K^+$  ions are sandwiched between trisilicate groups. A possible pathway for this conversion is also discussed.

## Introduction

One of the most demanding challenges in the field of separations science is the removal of highly radioactive species such as  $^{90}Sr^{2+}$  and  $^{137}Cs^+$  from nuclear waste. The waste streams may be 5–6 M in  $Na^+$  and either highly alkaline or highly acid and contain additional cationic and anionic species and possibly organic complexing agents.<sup>1</sup> To effect the required separations the design of special chelating resins,<sup>2</sup> complexants,<sup>3</sup> and/or highly selective ion exchange materials<sup>4</sup> are necessary. Removal of the high-level radioactive species and immobilization in glass will allow the bulk of the waste to be disposed of as a unit. This procedure will result in a considerable cost savings and minimize the storage space requirement for high-level waste.<sup>5</sup>

Inorganic ion exchangers, because of their high thermal and radiation stability, high selectivities, and ion exchange capacities,

have experienced a long history of involvement with radioactive processes and separations.<sup>6</sup> Much work was concentrated on layered phosphates<sup>6b,7</sup> and mixed phosphate–phosphonates,<sup>8</sup> but these exchangers hydrolyze extensively in strongly alkaline solutions. Similarly, zeolites are not stable in strong acid or base systems. However, when suitably protonated and for special wastes, they have served in practical applications.<sup>9</sup> Recently, we developed a sodium titanate exchanger,  $Na_4Ti_9O_{20}$ , that is highly specific for  $Sr^{2+}$  in strong alkaline solution.<sup>10</sup> This development was an outgrowth of studies initiated in Finland.<sup>11</sup>

Amorphous sodium titanates for use in nuclear waste separations were also under study at Sandia National Laboratory.<sup>12</sup> These studies eventually led to development of a sodium titanium silicate that is highly selective for cesium ions.<sup>13</sup>

- (6) (a) Ruvarac, A. L.; Clearfield, A. *J. Serb. Chem. Soc.* **1988**, *53*, 283 and references therein. (b) *Inorganic Ion Exchange Materials*; Clearfield, A., Ed.; CRC Press: Boca Raton, FL, 1982.
- (7) (a) Clearfield, A. *Comments Inorg. Chem.* **1990**, *10*, 114. (b) Clearfield, A. *Mater. Chem. Phys.* **1993**, *35*, 257.
- (8) Clearfield, A. In *New Developments in Ion Exchange*; Abe, M., Kataoka, T., Suyuki, T., Eds.; Kodansha: Tokyo, 1991; p 121.
- (9) Bray, L. A.; Hara, F. T. In *Proceedings of the First Hanford Separations Workshop*; Battelle, PNNL: Richland, WA, May 1993; p II 87.
- (10) Cahill, R. A. Ph. D. Dissertation, Texas A&M University.
- (11) (a) Lehto, J.; Heinonen, D. J.; Miettinen, J. K. *Radiochem. Radioanal. Lett.* **1981**, *46*, 381. (b) Heinonen, D. J.; Lehto, J.; Miettinen, J. K. *Radiochem. Acta* **1981**, *28*, 93. (c) Lehto, J.; Miettinen, J. K. *IAEA-TECDOC-337*; Int. Atomic Energy Agency: Vienna, 1985; p 9. (d) Lehto, J.; Clearfield, A. *J. Radioanal. Nucl. Chem. Lett.* **1987**, *118*, 1. (e) Clearfield, A.; Lehto, J. *Solid State Chem.* **1988**, *73*, 98.
- (12) Lynch, R. W.; Dosch, R. G.; Kenna, B. T.; Johnstone, J. K.; Nowak, E. J. In *IAEA-SM-207/75*; Int. Atomic Energy Agency: Vienna, 1976; p 361.

\* To whom correspondence should be addressed.

<sup>®</sup> Abstract published in *Advance ACS Abstracts*, June 1, 1997.

- (1) *Proceedings of the First Hanford Separation Science Workshop*; Battelle, PNL: Richland, WA; May 1993; PNL-SA-2175.
- (2) Chiarizia, R.; D'Arcy, K. A.; Horowitz, E. P.; Alexandratos, S. D.; Trochimcyuk, A. W. *Solvent Extr. Ion Exch.* **1996**, *14*, 519 and references therein.
- (3) (a) Dietz, M. L.; Horowitz, E. P.; Jensen, M. P.; Rhoads, S.; Bartsch, R. A.; Palka, A.; Krzykowski, Nam, J. *Solvent Extr. Ion Exch.* **1996**, *14*, 357. (b) Lumetta, G. J.; Wagner, M. J.; Carlson, C. D. *Solvent Extr. Ion Exch.* **1996**, *14*, 35.
- (4) Clearfield, A. In *Industrial Environmental Chemistry*; Sawyer, D. T., Martell, A., E.; Eds.; Plenum Press: New York, 1992; p 289.
- (5) Morsey, J. R.; Swanson, J. L. *A primer on Hanford Defence Tank Waste and Prospects for advanced Chemical Separations*; Battelle Pacific Northwest Laboratories: Richland, WA, April 1991.

Subsequent structural studies<sup>14</sup> showed that the compound has an ideal composition of Na<sub>2</sub>Ti<sub>2</sub>O<sub>3</sub>(SiO<sub>4</sub>)·2H<sub>2</sub>O and revealed details of the ion exchange process. The structure consists of tunnels running parallel to the *c*-axis but also cavities within the walls of the tunnels. Cesium ion fits perfectly within the tunnels but is too large to occupy the cavities within the tunnel framework. Thus, although the titanosilicate is highly selective for Cs<sup>+</sup>, in high alkaline solutions containing Na<sup>+</sup> and K<sup>+</sup> the capacity for Cs<sup>+</sup> is very low. The smaller cations occupy the framework sites and block the free diffusion of the larger Cs<sup>+</sup> ions.

As a part of our ongoing research, we have undertaken a systematic study of inorganic ion exchangers with layered or three-dimensional frameworks. Our primary aim is to elucidate their structures and, if necessary, to introduce chemical and structural modifications in order to achieve high capacity and selectivity for specific ionic or molecular species. Some new porous titanium phosphates<sup>15</sup> and titanium silicates<sup>16–18</sup> have recently been prepared and their structures solved by means of their X-ray diffraction data. In this paper we report the synthesis and X-ray powder structure of a novel framework compound based on zirconium trisilicate. The compound has high selectivity for Cs<sup>+</sup> ions while the analogous titanium compound does not. To understand this behavior we have prepared a number of ion exchanged phases of the zirconium trisilicate compound and studied their structures. These compounds, on heating, transform to a highly stable phase, analogous to the mineral wadeite. The cations in this high-temperature phase are strongly held in the lattice, and this property is important if such materials are to be used for removal and storage of radioactive species.

## Experimental Section

**Materials and Methods.** All reagents were of analytical grade (Aldrich) and used without further purification. Thermogravimetric analysis was carried out with a TA 4000 unit, at a heating rate of 10°C/min under a nitrogen atmosphere. The IR spectrum was recorded on a Perkin-Elmer 1720-X FTIR unit by the KBr disk method. The solids were dissolved in HF, and the zirconium and silicon contents were determined using a SpectraSpec DCP-AEC spectrometer. The K, Na, and Cs contents were determined using Varian Spectra AA-300 atomic absorption spectrometer.

**Synthesis of K<sub>2</sub>ZrSi<sub>3</sub>O<sub>9</sub>·H<sub>2</sub>O.** A 13.5 mL solution of 70% Zr(OC<sub>3</sub>H<sub>7</sub>) was mixed with 7 g of SiO<sub>2</sub> (dissolved in 45 mL of 4 M KOH solution). The mixture was placed in a 100 mL stainless steel Teflon vessel, and the reaction was carried out at 180 °C for 5 days. The solid white product was filtered out, washed with distilled water, and air dried. Anal. Found: Zr, 21.85; Si, 20.15; K, 18.75. Calc for K<sub>2</sub>ZrSi<sub>3</sub>O<sub>9</sub>·H<sub>2</sub>O: Zr, 21.93; Si, 20.24; K, 18.80.

The potassium trisilicate, thus obtained, was treated with an excess of 2 M NaCl solution to obtain the sodium form, Na<sub>2</sub>ZrSi<sub>3</sub>O<sub>9</sub>·H<sub>2</sub>O (Anal. Found: Zr, 23.75; Si, 22.00; Na, 12.10. Calc: Zr, 23.76; Si, 21.93; Na, 12.01). The K and Na forms were then ion exchanged with different amounts of Cs to get the Cs phases. Compound **2**, K<sub>0.9</sub>Cs<sub>1.1</sub>-ZrSi<sub>3</sub>O<sub>9</sub>·H<sub>2</sub>O, was prepared from 1 g of compound **1** by treatment with 200 mL of a 0.5 M CsCl solution at pH 10.0 (Anal. Found: Zr, 17.60; Si, 16.20; K, 6.75; Cs, 28.20. Calc: Zr, 15.55; Si, 16.20; K, 6.77; Cs, 28.22). Compound **2** was converted to compound **3**, K<sub>0.5</sub>Cs<sub>1.5</sub>-ZrSi<sub>3</sub>O<sub>9</sub>·H<sub>2</sub>O, (Anal. Found: Zr, 16.50; Si, 15.23; K, 3.90; Cs, 35.00.

Calc: Zr, 16.37; Si, 15.11; K, 3.51; Cs, 35.88), by additional treatment with CsCl solution. Compound **5**, Na<sub>0.98</sub>Cs<sub>1.02</sub>ZrSi<sub>3</sub>O<sub>9</sub>·H<sub>2</sub>O, was obtained from Na<sub>2</sub>ZrSi<sub>3</sub>O<sub>9</sub>·H<sub>2</sub>O by treatment with 200 mL of CsCl (0.05 M) solution at pH 10.5 (Anal. Found: Zr, 19.32; Si, 17.83; Na, 5.86; Cs, 22.59. Calc: Zr, 18.38; Si, 16.96; Na, 4.55; Cs, 27.39). Compound **6**, Na<sub>0.6</sub>Cs<sub>1.4</sub>ZrSi<sub>3</sub>O<sub>9</sub>·H<sub>2</sub>O, was prepared from compound **5** by additional treatment with CsCl solutions. Anal. Found: for **6**: Zr, 16.95; Si, 15.60; Na, 2.55; Cs, 34.65. Calc: Zr, 16.95; Si, 15.64; Na, 2.57; Cs, 34.67.

**X-ray Data Collection.** X-ray powder data for the samples were collected using a flat aluminum sample holder by means of a Rigaku computer automated diffractometer. The X-ray source was a rotating anode operating at 50 kV and 180 mA with a copper target and graphite-monochromated radiation. Data were collected at room temperature between 10 and 85°, in 2θ with a step size of 0.01° and a count time of 10 s per step. For compound **3** data were collected up to 100° in 2θ using the same step size and count time. Subsequently, data for the samples were collected by using an aerosol suspension chamber<sup>19a</sup> to evaluate the influence of preferred orientation effects. A comparison of these data sets to those collected by the regular side loading method showed only minor affects in the intensity patterns due to preferred orientation, and therefore, the data sets obtained by regular methods were used in subsequent calculations. The powder patterns were indexed by Ito methods.<sup>19b</sup> For compound **1**, a solution with figure of merit of 117 indicated an orthorhombic unit cell with *a* = 10.287, *b* = 13.30, and *c* = 7.19 Å. Similar solutions were obtained for the ion-exchanged phases: Compound **2**, *a* = 10.557, *b* = 13.42, *c* = 7.35 Å (FOM = 75); compound **3**, *a* = 10.63, *b* = 13.46, *c* = 7.36 Å (FOM = 44); compound **4**, *a* = 10.48, *b* = 13.37, *c* = 7.26 Å (FOM = 48); compound **5**, *a* = 10.70, *b* = 13.40, *c* = 7.36 Å (FOM = 99); compound **6**, *a* = 10.69, *b* = 13.42, *c* = 7.37 Å (FOM = 44). The systematic absences in these compounds were consistent with the space group P2<sub>1</sub>2<sub>1</sub>2<sub>1</sub>.

**Structure Solution and Refinement.** The structure factor amplitudes for compound **1** were extracted from the profile using decomposition methods.<sup>20</sup> This procedure yielded 73 peaks with 62 single indexed reflections and the remaining with two contributing reflections. The intensities of the latter set of peaks were divided equally between the contributing reflections and included in the starting data set. This data set was converted to a single crystal type data set (*F*<sub>hkl</sub>, *σ*<sub>hkl</sub>) and input to a "direct methods program", MITHRIL,<sup>21</sup> in the TEXAN<sup>22</sup> series of programs. An *E*-map calculated for a solution with the best figure of merit (Abs FOM = 2, Psi Zero = 1.4, and Resid = 19.39) revealed the positions of Zr, 2 Si, 2 K, and 3 O atoms.

In a second method, the X-ray powder pattern was decomposed using a more sophisticated algorithm, viz. the Le Bail method in GSAS.<sup>23</sup> Using a random atom position as a structural model, Rietveld refinement was carried out on the basis of the correct unit cell dimensions and the space group symmetry. The parameters refined were terms for background function, unit cell parameters, zero point error, and profile coefficients. The refinement converged with *R*<sub>wp</sub> = 0.075 and *R*<sub>p</sub> = 0.053. The extraction procedure yielded 462 independent reflections in the 2θ range 10–80°. This data set was input to the above mentioned direct methods program and the best solution (Abs FOM = 1.67, Psi Zero = 1.28, Resid = 30) revealed the positions of Zr, 2 Si, 2 K, and 5 oxygen atoms in the *E*-map. Note that the number of atoms located from the *E*-map was nearly the same in the two attempts although a significantly higher number of reflections were used in the second method.

The structural model thus obtained was used for Rietveld refinement of the full pattern. After the initial refinement of scale, background function, unit cell parameters, and profile parameters, the atomic positions were refined with soft constraints only for the trisilicate

(13) Anthony, R. G.; Philip, C. V.; Dosch, R. G. *Waste Mgt.* **1993**, *13*, 503.

(14) (a) Poojary, D. M.; Cahill, R. A.; Clearfield, A. *Chem. Mater.* **1994**, *6*, 2364. (b) Poojary, D. M.; Bortun, A. I.; Bortun, L. N.; Clearfield, A. *Inorg. Chem.* **1996**, *35*, 6131.

(15) Poojary, D. M.; Bortun, A. I.; Bortun, L. N.; Clearfield, A. *J. Solid State Chem.*, in press.

(16) Chapman, D. M.; Roe, A. L. *Zeolites* **1990**, *10*, 730.

(17) Behrens, E. A.; Poojary, D. M.; Clearfield, A. *Chem. Mater.* **1996**, *8*, 1244.

(18) Roberts, M. A.; Fitch, A. N. *Z. Kristallogr.* **1996**, *211*, 378.

(19) (a) Davis, B. L. *Powd. Diff.* **1986**, *1*, 240. (b) Visser, J. W. *Appl. Crystallogr.* **1969**, *2*, 89.

(20) Rudolf, P. R.; Clearfield, A. *Acta Crystallogr.* **1985**, *B41*, 418.

(21) Gilmore, G. J. *J. Appl. Crystallogr.* **1984**, *17*, 42.

(22) TEXSAN: *Structure Analysis Package*; Molecular Structure Corp. The Woodlands, TX, 1987.

(23) Larson, A.; von Dreele, R. B. *GSAS: Generalized Structure Analysis System*, LANSCE; Los Alamos National Laboratory; copyright 1985–88 by the Regents of the University of California.

**Table 1.** Crystallographic Data for the Zirconium Trisilicate Phases<sup>a</sup>

	1	2	3	4	5	6
fw	415.68	518.87	556.39	383.46	495.55	537.35
space group	$P2_12_12_1$	$P2_12_12_1$	$P2_12_12_1$	$P2_12_12_1$	$P2_12_12_1$	$P2_12_12_1$
<i>a</i> (Å)	10.2977(2)	10.5589(2)	10.6289(2)	10.4855(3)	10.6710(3)	10.6895(2)
<i>b</i> (Å)	13.3207(3)	13.4237(3)	13.4599(2)	13.3714(3)	13.3921(3)	13.4316(3)
<i>c</i> (Å)	7.1956(1)	7.3510(2)	7.3591(1)	7.3592(2)	7.3537(2)	7.3706(1)
<i>V</i> (Å <sup>3</sup> )	987.05(4)	1041.9(1)	1052.8(1)	1017.8(1)	1050.9(1)	1058.2(1)
<i>Z</i>	4	4	4	4	4	4
<i>d</i> <sub>calc</sub> (g/cm <sup>3</sup> )	2.797	3.308	3.510	2.502	3.131	3.372
no. of reflns	426	476	655	456	461	464
<i>R</i> <sub>wp</sub> <sup>b</sup>	0.072	0.067	0.061	0.059	0.061	0.065
<i>R</i> <sub>p</sub>	0.051	0.050	0.046	0.043	0.046	0.050
<i>R</i> <sub>F</sub>	0.041	0.051	0.042	0.073	0.043	0.043

<sup>a</sup> Formulas: (1)  $K_2ZrSi_3O_9 \cdot H_2O$ ; (2)  $K_{0.9}Cs_{1.1}ZrSi_3O_9 \cdot H_2O$ ; (3)  $K_{0.5}Cs_{1.5}ZrSi_3O_9 \cdot H_2O$ ; (4)  $Na_2ZrSi_3O_9 \cdot H_2O$ ; (5)  $Na_{0.98}Cs_{1.02}ZrSi_3O_9 \cdot H_2O$ ; (6)  $Na_{0.6}Cs_{1.4}ZrSi_3O_9 \cdot H_2O$ . <sup>b</sup> See ref 23 for definitions.

**Table 2.** Positional and Thermal Parameters for  $K_2[ZrSi_3O_9] \cdot H_2O$ 

	<i>x</i>	<i>y</i>	<i>z</i>	<i>U</i> <sub>iso</sub> , <sup>b</sup> Å <sup>2</sup>
Zr1	0.4475(2)	0.2101(2)	0.2586(4)	0.028(2)
Si1	0.1771(5)	0.1735(4)	0.0066(8)	0.012(3)
Si2	0.0277(5)	0.0476(3)	0.7314(9)	0.011(2)
Si3	0.6361(6)	0.3320(5)	0.5799(8)	0.027(4)
O1	0.4140(6)	0.3674(4)	0.2452(12)	0.011(5)
O2	0.3283(6)	0.1897(6)	0.0316(9)	0.018(6)
O3	0.5028(7)	0.0631(4)	0.2663(12)	0.009(5)
O4	0.5618(8)	0.2380(5)	0.4953(9)	0.035(6)
O5	0.6075(6)	0.2307(5)	0.0845(10)	0.031(7)
O6	0.2920(6)	0.1877(6)	0.4359(10)	0.002(6)
O7	0.1011(7)	0.1522(6)	0.2019(8)	0.008(5)
O8	0.0938(8)	0.0652(5)	0.5247(10)	0.006(6)
O9	0.1497(7)	0.0768(6)	0.8752(11)	0.027(6)
K1(M1)	0.2112(6)	0.6320(4)	0.1533(8)	0.044(3)
K2(M2)	0.4269(5)	0.0783(3)	0.7147(8)	0.020(2)
O1O(M3) <sup>a</sup>	0.6887(12)	0.0607(8)	0.8650(17)	0.004(5)

<sup>a</sup> Water oxygen atom. <sup>b</sup>  $U_{iso} = B_{iso}/8\pi^2$ .

groups. A series of difference Fourier maps were then calculated which allowed the positioning of the remaining atoms in the structure. The full structure was then refined with the above mentioned soft constraints. In the final stages of refinement the weights of these constraints were reduced and kept at a value necessary to maintain a satisfactory geometry for the trisilicate group. The preferred orientation factor was refined to a value very close to 1.0. The diffraction vector is along the *c*\* axis, and the ratio of the effect along this axis to that along the perpendicular plane was refined. All the atoms were refined isotropically. Neutral atomic scattering factors, as stored in GSAS, were used for all atoms. No corrections were made for absorption.

Refined positions of the Zr trisilicate group in compound **1** were used as the starting model for the structure solution of compounds **2–6**. The charge neutralizing cations and water molecules were located in difference Fourier maps following the initial Rietveld refinement. The structure refinements were carried out in a manner similar to that described above for compound **1**.

Crystallographic and experimental parameters are given in Table 1. Final positional and thermal parameters for compound **1** are given in Tables 2, and the positional parameters for the lattice sites for compounds **2–6**, in Table 3. Bond lengths are shown in Table 4. The bond parameters concerning the cations are given in Table 5. The final Rietveld refinement difference plot for compound **1** is given in Figure 1.

## Results

**Structure of  $K_2ZrSi_3O_9 \cdot H_2O$ .** The structure consists of two independent cationic positions, a Zr atom, a water molecule, and a trisilicate group in the asymmetric unit. The trisilicate group,  $Si_3O_9^{6-}$  exists as a linear chain polymer and therefore could be better represented as  $[-O-SiO_2-]_n^{2n-}$ . Silicon atom Si1 is connected to Si2 through O9, and Si2 is linked to Si3 by O8. Oxygen O7 then links Si3 to Si1, and hence, the polymeric chain extends infinitely. The axis of this polymer is oriented

approximately along the *c*-axis of the crystal. The silicate chains are linked together by the Zr atoms. A portion of the polymeric trisilicate chains and their connectivity to the Zr atoms is shown in Figure 2. This figure also clearly shows the six-membered rings formed by the trisilicate groups about the metal atoms Zr1. The sizes of the rings mentioned here and in the following section take into account all the involved atoms including the oxygens. One of the trisilicate groups forms two adjacent six-membered rings about Zr1, involving all three monomeric silicates, and provides three binding sites for the Zr atoms, which are O4, O1, and O5 in this case. The polymer chain on the other side of the metal atom forms only one six-membered ring involving oxygen atoms O2 and O6 of silicon atoms Si1 and Si3, respectively. The remaining coordination site of the metal octahedron comes from an oxygen (O3) from the trisilicate chain shifted along the *b*-axis of the crystal. This linkage thus leads to a three-dimensional network for the compound.

The structure is significant in that it contains channels similar to those found in zeolites but formed from alternating silicate tetrahedra and metal octahedra as in the case of some porous titanium silicate compounds.<sup>14,24</sup> The channels run along the *c*-axis, and they possess 16-membered ring openings as shown in Figure 3. The rings are formed by four Zr atoms which are interconnected by  $-Zr-O-Si-O-Zr-$  type linkages. It may be noted that these rings are not exactly in the *ab*-plane; instead they are tilted with respect to the *c*-axis. Any one such channel is surrounded by four similar channels (Figure 4), all running along the same direction (*c*-axis). These are connected to each other, in the perpendicular direction to the channel direction which is approximately along the [110] diagonal, through 14-membered ring openings, as shown in Figure 2. The ring is fairly large, and it involves unit cell translated Zr atoms (along the *c*-axis;  $\sim 7.2$  Å) bridged on either side by the silicate groups. The total channel system in the structure therefore has three-dimensional openings in character.

The structure also possess a second set of channels that have smaller openings than the larger 16-atom type of channels described above. These smaller channels have 12-membered ring openings consisting of two Zr atoms linked by disilicate groups on either side. These channels also run along the *c*-axis parallel to the large ones and alternate with them. Thus, each large channel in the structure is surrounded by four 16-membered ring channels and four 12-membered ring channels as shown in the ball and stick representation in Figure 4. The

(24) (a) Kuznicki, S. M. U.S. Pat. 4 853 202, 1989, 916. (b) Kuznicki, S. M.; Thrush, K. A.; Allen, F. M.; Levine, S. M.; Hamel, M. M.; Hayhurst, D. T.; Maknoud, M. In *Synthesis of Microporous Materials*; Ocelli, M., Robson, H., Eds.; Van Nostrand Reinhold: New York, 1992; Vol. 1, p 427. (c) Valtchev, V. P. *J. Chem. Chem. Soc., Chem. Commun.* **1994**, 261.

**Table 3.** Positional Parameters for the Sites M1, M2, and M3 in Structures 2–6

site	position	2	3	4	5	6
M1	x	0.2416(18)	0.2557(15)	0.2727(16)	0.2388(15)	0.2461(17)
	y	0.5782(10)	0.5718(10)	0.5603(10)	0.5600(8)	0.5626(9)
	z	−0.0002(24)	−0.0355(22)	−0.0432(20)	0.0039(15)	0.0119(19)
	occ	0.7 K; 0.3 O	0.5 K; 0.5 O	Na	0.8 Na; 0.1 O; 0.1 Cs	0.6 Na; 0.3 O; 0.1 Cs
M2	x	0.4388(2)	0.4353(2)	0.4478(13)	0.4403(2)	0.4334(2)
	y	0.0837(1)	0.0837(1)	0.1007(8)	0.0824(1)	0.0831(1)
	z	0.7530(10)	0.7530(7)	0.756(5)	0.7533(9)	0.7497(8)
	occ	0.8 Cs; 0.2 K	Cs	Na	0.82 Cs; 0.18 Na	Cs
M3	x	0.8022(7)	0.7999(3)	0.8448(19)	0.8088(8)	0.8053(6)
	y	0.1228(5)	0.1239(2)	0.1356(13)	0.1140(6)	0.1258(4)
	z	0.1932(12)	0.2126(7)	0.156(4)	0.1693(13)	0.2105(14)
	occ	0.3 Cs; 0.7 O	0.5 Cs; 0.5 O	O	0.1 Cs; 0.9 O	0.3 Cs; 0.7 O

**Table 4.** Bond Lengths (Å) for the Zirconium Trisilicate Framework

bond	compound					
	1	2	3	4	5	6
Zr1–O1	2.126(5)	2.141(4)	2.142(4)	2.133(5)	2.134(4)	2.125(4)
Zr1–O2	2.061(5)	2.075(5)	2.083(4)	2.074(5)	2.072(5)	2.081(5)
Zr1–O3	2.040(5)	2.016(4)	2.017(4)	2.003(5)	2.010(4)	2.019(4)
Zr1–O4	2.103(5)	2.086(5)	2.080(4)	2.078(5)	2.090(4)	2.082(5)
Zr1–O5	2.088(5)	2.093(5)	2.102(4)	2.077(5)	2.083(5)	2.091(5)
Zr1–O6	2.068(5)	2.077(5)	2.069(4)	2.081(5)	2.087(5)	2.079(5)
Si1–O2	1.583(6)	1.636(6)	1.643(6)	1.641(6)	1.640(6)	1.648(6)
Si1–O5	1.604(6)	1.599(6)	1.599(5)	1.612(6)	1.607(5)	1.610(5)
Si1–O7	1.633(6)	1.613(6)	1.609(5)	1.594(6)	1.613(5)	1.618(5)
Si1–O9	1.623(6)	1.617(6)	1.623(5)	1.624(6)	1.628(5)	1.619(5)
Si2–O1	1.637(6)	1.635(6)	1.637(5)	1.621(6)	1.642(5)	1.649(5)
Si2–O3	1.528(6)	1.551(5)	1.570(4)	1.559(5)	1.557(4)	1.565(5)
Si2–O8	1.652(6)	1.666(6)	1.661(5)	1.664(6)	1.656(5)	1.655(6)
Si2–O9	1.673(6)	1.653(6)	1.651(5)	1.639(6)	1.653(6)	1.654(6)
Si3–O4	1.589(6)	1.603(6)	1.609(5)	1.613(6)	1.599(5)	1.608(5)
Si3–O6	1.631(7)	1.637(6)	1.644(6)	1.621(6)	1.642(6)	1.649(6)
Si3–O7	1.624(6)	1.614(6)	1.608(5)	1.625(6)	1.617(5)	1.612(5)
Si3–O8	1.623(7)	1.605(6)	1.611(5)	1.604(6)	1.626(5)	1.619(5)

view in this figure is down the *c*-axis. The pore openings of the large and small channels can be seen as distorted octagons and hexagons, respectively. The small channels cannot have ion diffusion along the *c*-axis as the direction is blocked by neighboring oxygens (O9–O8') positioned at about 3.6 Å apart. Because of this close contact the pore is divided into two separate cavities. These cavities themselves have restricted openings; however, they are opened to the large channels both along the *a*-axis direction and along the [110] direction. The opening along the diagonal direction is shown in Figure 5 and is a large 24 atom ring. Along the *a*-axis, these cavities open to larger ones by rings consisting of four Zr atoms, connected by monomeric silicates, and dimeric silicates approximately along the *b*- and *c*-directions, respectively. Thus a given small cavity is accessible to two neighboring large channels.

For simplicity, the two cationic positions K1 and K2 in the structure of K<sub>2</sub>ZrSi<sub>3</sub>O<sub>9</sub>·H<sub>2</sub>O are respectively designated as site M1 and site M2. The water oxygen O10 is partially replaced by Cs atoms on ion exchange and therefore this site is designated as M3 in the following discussions. The K<sup>+</sup> ion K1 (site M1) and water oxygen O10 (site M3) are located in the large pore. The water oxygen in this case is hydrogen bonded (Table 5) to two silicate oxygens, O1 and O5. It is also bonded to K1 with a K1–O10 distance of 2.58 Å. K1 is surrounded by six oxygens (O1, O3, O4, O5, O6, and O10) and the corresponding K–O bond distances are in the range 2.6–3.2 Å. The K<sup>+</sup> ion K2 (site M2) occupies the cavities formed within the small channels. This ion cannot diffuse to the same sites in the neighboring cavity because of the barrier created by the adjacent oxygens of the silicate groups as described earlier. K2 ions, however, have free access to the large pores that are occupied by ions or water oxygens at sites M1 and M3. Unlike K1, K2 is bonded

**Table 5.** Selected Contacts (Å) for the Cations and Water Molecules

	1	2	3	4	5	6
Cation M1						
M1–O1	3.21(1)	2.62(2)	2.59(2)	2.78(2)	2.75(1)	2.82(2)
M1–O2	3.64(1)					
M1–O3	3.14(1)	3.42(2)	3.51(2)	3.23(2)		
M1–O4	2.93(1)	2.78(2)	2.82(2)	2.74(2)	2.93(2)	2.89(2)
M1–O5	2.96(1)					
M1–O6	2.87(1)	3.07(2)	3.14(2)	3.46(2)		
M1–O10	2.58(1)	3.12(2)	2.98(2)	3.17(2)	2.76(1)	2.28(2)
		2.38(2)	2.55(2)	2.87(2)	2.56(1)	3.1(1)
Cation M2						
M2–O2	2.90(1)	3.05(1)	3.08(1)	2.86(3)	3.08(1)	3.10(1)
M2–O3	3.33(1)	3.74(1)	3.74(1)	3.64(4)	3.73(1)	3.73(1)
		3.70(1)	3.70(1)	3.78(4)	3.68(1)	3.71(1)
M2–O4	2.99(1)	3.37(1)	3.38(1)	3.30(3)	3.39(1)	3.39(1)
M2–O5		3.27(1)	3.27(1)	3.04(3)	3.26(1)	3.30(1)
M2–O6	2.84(1)	3.03(1)	3.05(1)	2.82(3)	3.07(1)	3.05(1)
M2–O7	3.09(1)	3.31(1)	3.30(1)		3.35(1)	3.33(1)
		3.85(1)	3.91(1)		3.84(1)	3.88(1)
M2–O8	2.95(1)	3.47(1)	3.44(1)	3.46(2)	3.35(1)	3.42(1)
		3.32(1)	3.34(1)	3.49(3)	3.48(1)	3.37(1)
M2–O9	3.08(1)	3.57(1)	3.53(1)	3.34(3)	3.26(1)	3.24(1)
	2.30	3.24(1)	3.28(1)		3.58(1)	3.54(1)
Cation M3/H <sub>2</sub> O						
M3–O1	2.63(1)	3.51(1)	3.66(1)	3.14(3)	3.34(1)	3.63(1)
M3–O2		3.02(1)	3.08(1)	2.82(2)	2.96(1)	3.02(1)
M3–O3		3.46(1)	3.51(1)		3.64(1)	3.63(1)
M3–O4		3.29(1)	3.22(1)		3.45(1)	3.24(2)
M3–O5	2.89(1)	2.98(1)	3.05(1)	3.14(2)	3.01(1)	3.06(1)
M3–O6		3.56(1)	3.43(1)		3.72(1)	3.40(1)
M3–O7		3.26(1)	3.30(1)	2.911(2)	3.34(1)	3.28(1)

to 8 oxygen atoms, all of them from the silicate groups. Apart from the terminal oxygens (O2, O3, O4, and O6), the oxygens of the Si–O–Si bridge (O7, O8, and O9) also participate in cation binding. The K2–O bond distances are in the range 2.3–3.3 Å, with the shortest bond being to O9.

**Cs-Exchanged Phases of K<sub>2</sub>ZrSi<sub>3</sub>O<sub>9</sub>·H<sub>2</sub>O.** The structures of the Cs exchanged phases are isomorphous with K<sub>2</sub>ZrSi<sub>3</sub>O<sub>9</sub>·H<sub>2</sub>O (**1**). Accordingly, the description of the three-dimensional structure of the Zr trisilicate framework is similar to that described for compound **1**. The uptake of Cs, however, resulted in the expansion of unit cell dimensions, particularly the *a*- and *c*-axes. The major difference in these phases is concerned with respect to the distribution of cations and water molecules among the three lattice positions, described below.

Compound **1** consists of two exchangeable potassium ions. Our primary interest is to see whether these cations can selectively be replaced by Cs<sup>+</sup> ions without much structural distortion. In order to understand the exchange reactions, the K ions were replaced in steps and their structures examined by the application of Rietveld methods to their powder diffraction data. Since the two cationic sites M1 and M2 have different environments in the structure, partial exchange of ions would

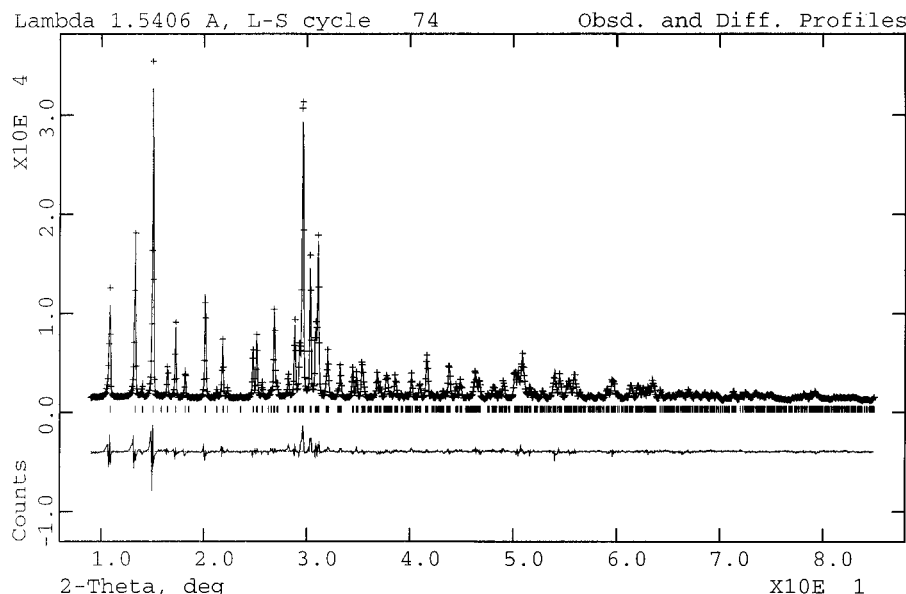


**Figure 1.** Observed (+) and calculated (−) profiles for the Rietveld refinement for  $K_2ZrSi_3O_9 \cdot H_2O$ . The bottom curve is the difference plot on the same intensity scale.

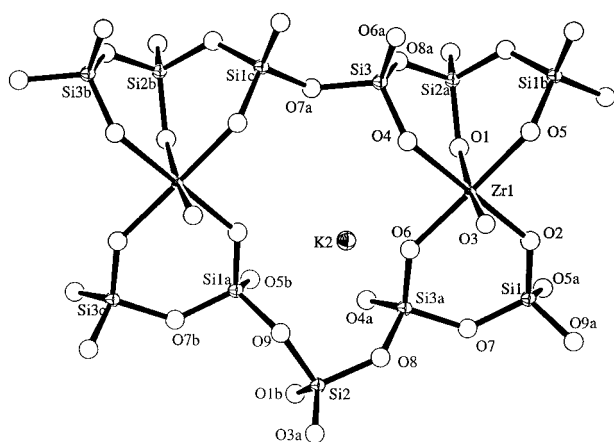


**Figure 2.** Section of the structure of compound **1** showing the atom labeling and coordination about the zirconium atom. The linkage of the Zr atoms through the linear chain polymers of trisilicate group is also shown. The view is approximately along the [110] direction, and the *c*-axis is horizontal.

shed light on the selectivity of  $Cs^+$  ions between these two sites. In the initial attempt, about 50% of the  $K^+$  ions in compound **1** were exchanged for  $Cs^+$  to obtain a partially exchanged phase, compound **2**. Compound **2** was then treated with additional  $Cs^+$  ion solution to obtain compound **3** in which about 75% of the cationic sites are filled by  $Cs^+$  ions.

In the initial stages of structure analysis of compound **2**, the Zr trisilicate framework was idealized by refinement of the groups obtained from compound **1** against the new unit cell parameters. Difference Fourier maps, as expected, revealed three lattice positions close to sites M1, M2, and M3. The electron densities at these sites, however, did not correspond to the occupancies of a particular ion or water oxygen. The density at site M2 was substantially high, and those at sites M1 and M3 were nearly the same and corresponded to about 50% of the density obtained for site M2. Therefore, initially the site M2 was assigned to  $Cs^+$  ions and sites M1 and M3 for K and water oxygen, respectively. After the positions of these sites were stabilized, their occupancies were refined. The occupancy at site M2 was refined to about 0.9 for  $Cs^+$  ions, and site M1 to about 0.83 for  $K^+$  ions, and surprisingly, the water site showed much higher density than expected for a water oxygen

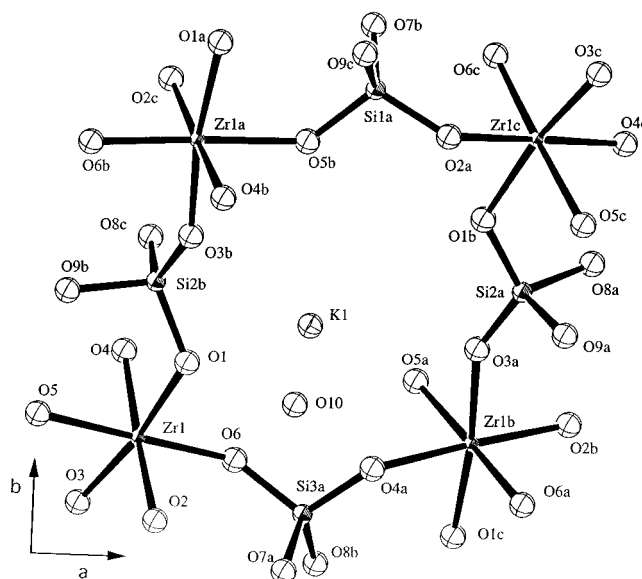


**Figure 3.** Arrangement of one of the cations and a water oxygen in the large pore formed from Zr-silicate bridging. The view is approximately along the *c*-axis.

atom. Subsequently site M3 was assigned Cs scattering factors and the occupancy was refined. The population parameter at this site corresponded to about 0.41 for Cs. On the basis of these data, site M2 was assigned 0.8 Cs occupancy and 0.2 K occupancy. Site M1 has 0.7 K occupancy and 0.3 water oxygen occupancy. Site M3 contains 0.3  $Cs^+$  ions and 0.7 water oxygen. This arrangement thus leads to the formula  $K_{0.9}Cs_{1.1}ZrSi_3O_9 \cdot H_2O$ , which is in very good agreement with the analytical data. This distribution of ions and the water oxygen atom at sites M1 and M3 should also satisfy reasonable cation-water contacts and avoid cation-cation contacts when the sites are replaced by cations. The formula given above satisfies these criteria as well. When site M3 is occupied by  $Cs^+$  ions (0.3), the neighboring site M1 is filled with water. In this arrangement, the closest M2-M3 distance of 3.24 Å is reasonable for a Cs-O bond length. In the absence of  $Cs^+$  ion, the site M3 is occupied by water oxygen and the site M2 is filled with  $K^+$  ions. Again the above mentioned M2-M3 distance is within the allowable K-O bond lengths.

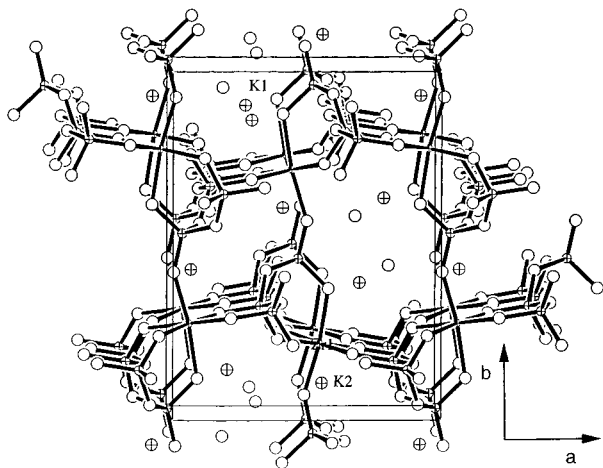


**Figure 4.** View of the structure of compound **1** showing the two types of channels in the structure. The open circles and crossed circles in the channels represent water oxygen and cations, respectively. Potassium ion K1 is located in the large channel, and K2 is in the small channel. The pairs of ions in the channels are due to the  $2_1$  axis along the  $c$ -axis.

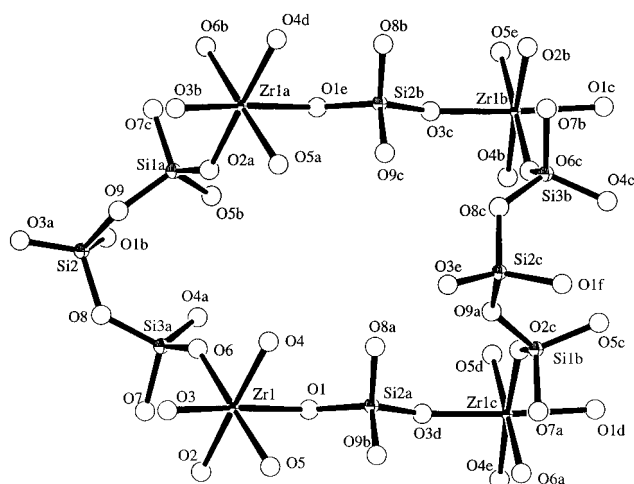


**Figure 5.** Zr-trisilicate connections approximately along the  $[110]$  direction showing the opening of the M2 site to the large channel. The  $b$ -axis is horizontal.

Additional loading of Cs<sup>+</sup> ions into compound **2** results in only minor changes in unit cell dimensions (Table 1) when compared to the changes observed between compound **1** and compound **2**. Rietveld analysis and occupancy refinement of compound **3** indicate that the site M2 is fully occupied by Cs<sup>+</sup> ions in this case. The site M1 is occupied equally by water oxygen and K<sup>+</sup> ions. Similarly the site M3 was found to have 0.5 occupancies each for both Cs and water. The formula K<sub>0.5</sub>Cs<sub>1.5</sub>ZrSi<sub>3</sub>O<sub>9</sub>·H<sub>2</sub>O for compound **3** thus derived is in good agreement with the results from the analytical data. Again as described for compound **2**, the arrangement of ions and water oxygen at sites M2 and M3 satisfy the stereochemical aspects. When Cs<sup>+</sup> ions occupy site M3, the corresponding atom type at site M1 is water oxygen. Similarly the site M3 is occupied by water oxygen when M1 is occupied by K<sup>+</sup> ions. In this case, the closest M2–M3 distance is 3.28 Å, which is reasonable for a strong Cs–O bond and is also acceptable for a K–O bond length.

**Structure of Na<sub>2</sub>ZrSi<sub>3</sub>O<sub>9</sub>·H<sub>2</sub>O (4).** The sodium phase of the Zr trisilicate was obtained from the potassium phase (compound **1**) by ion exchange. The sample thus obtained is less crystalline compared to the potassium phase. However, the data were sufficient to reveal the key structural features including the cationic and water oxygen positions. The oc-

cupancy refinement results indicate that almost all the potassium ions were exchanged for the Na<sup>+</sup> ions. The presence of sodium ions resulted in expansion of the unit cell dimensions notably along the  $a$ - and  $c$ -directions (Table 1). The Zr trisilicate framework and the cationic position at site M2 in this case is very similar to that found for the pure K phase. Significant changes, however, have resulted in the positions corresponding to the sites M1 and M3. The site M1 in the Na phase has shifted mostly along the  $c$ -direction by about 1.4 Å relative to the corresponding K<sup>+</sup> ion position in the K-phase. The position of the water oxygen is shifted in all the crystallographic directions, but again the shift is greatest along the  $c$ -direction (about 2.1 Å). The Na<sup>+</sup> ions and the water oxygens are less ordered compared to the ions and water oxygen in the pure K phase. The Na–O contacts at site M1 are all more than 2.8 Å, well above the Na–O optimal bond lengths. Consequently, the temperature factor for this Na<sup>+</sup> ion is notably high and moderately high for Na2. The contacts involving the water oxygen and the framework oxygens are different in the K and Na phases. In the K phase the water molecule has two hydrogen-bonding contacts with oxygens O1 (2.63 Å) and O5 (2.89 Å). Apart from these two contacts that are now at 3.14 Å, the water molecule in the Na phase is involved in two other contacts: one with O2 (2.82 Å) and the other with O7 (2.91 Å).

**Cs-Exchanged Phases of Na<sub>2</sub>ZrSi<sub>3</sub>O<sub>9</sub>·H<sub>2</sub>O.** As in the case of compound **1**, the cations in compound **4** were exchanged for Cs ions in two steps. Initially about 50% of the Na<sup>+</sup> ions in compound **4** were exchanged for Cs<sup>+</sup> to obtain compound **5**. Additional loading of Cs<sup>+</sup> into compound **5** resulted in compound **6**. These ion-exchanged phases were structurally characterized from their powder diffraction data. The positions of ions and water oxygens were derived from Fourier difference maps, and their contents at the lattice sites were derived from occupancy refinements.

In the 50% Cs-exchanged phase (compound **5**), the site M2 is occupied by about 0.82 Cs<sup>+</sup> ions and 0.18 by Na<sup>+</sup> ions. The distribution of ions at this site is very similar to that observed for compound **2**. However, in the present case, the electron density at site M3 is much lower and corresponds to only about 0.1 Cs occupancy. In the absence of Cs<sup>+</sup> ion, this site is filled with water oxygen (occupancy = 0.9). Interestingly, the remaining Cs<sup>+</sup> ions go to the site M1 which in the case of compounds **2** and **3** is occupied by either K<sup>+</sup> ions or water oxygens only. The site M1 in compound **5** is found to be occupied by Cs, Na, and water with occupancies of 0.1, 0.8, and 0.1, respectively. Thus the formula derived from X-ray data is Na<sub>0.98</sub>Cs<sub>1.02</sub>ZrSi<sub>3</sub>O<sub>9</sub>·H<sub>2</sub>O. The analytical data, however, indicated a formula Na<sub>1.2</sub>Cs<sub>0.8</sub>ZrSi<sub>3</sub>O<sub>9</sub>·H<sub>2</sub>O corresponding to a lower level of Cs exchange. When the site M1 is occupied by either Cs<sup>+</sup> or Na<sup>+</sup> ions (total = 0.9 occupancy for cations), the site M3 is filled with water oxygen. Only when site M3 is occupied by Cs<sup>+</sup> ions is water present in site M1. As in the case of compounds **2** and **3**, the observed M2–M3 distance of 3.24 Å is acceptable either for K–O or Cs–O bond lengths.

The distribution of ions and water oxygens at the lattice sites found for compound **5** was confirmed from the structure analysis of compound **6** in which additional Na<sup>+</sup> ions were replaced by Cs<sup>+</sup> ions. These additional Cs<sup>+</sup> ions go only to sites M3 and M2 and not to M1. The formula derived for compound **6** from the structural study is Na<sub>0.6</sub>Cs<sub>1.4</sub>ZrSi<sub>3</sub>O<sub>9</sub>·H<sub>2</sub>O and is in excellent agreement with the analytical data. The site M2 in this case is fully occupied by the Cs<sup>+</sup> ion. Water oxygen and Cs<sup>+</sup> ions occupy the site M3 with population parameters of about 0.7 and 0.3, respectively. The site M1, as in the case of compound

5, is occupied by Na<sup>+</sup> ion, Cs<sup>+</sup> ion, and water oxygen. The total cation occupancy at this site is 0.7 consisting of 0.1 for Cs<sup>+</sup> and 0.6 for Na<sup>+</sup> ion. When these ions are present at the M1 site, M3 is filled with water. The water occupancy at M1 is 0.3 and it exists when Cs<sup>+</sup> ions are present at site M3. The M2–M3 distance (3.24 Å) is similar to that found for other Cs-exchanged phases of both K and Na zirconium silicates.

### Discussion

A comparison of the unit cell dimensions given in Table 1 shows that, contrary to expectation, the pure Na phase has slightly larger dimensions than that of the pure K phase. These changes have not affected the ZrSi<sub>3</sub>O<sub>9</sub><sup>2-</sup> framework structure in these two phases. However, the differences are apparent in the location of one of the cation positions and the water oxygen position. The cation position M2 remains unchanged in all the compounds including the Cs-exchanged phases. This position, as described above, is highly selective for Cs<sup>+</sup> ions. The sites M1 and M3 in compound **1** shift significantly on Cs<sup>+</sup> exchange. These new positions are also very similar to the corresponding sites in compounds **5** and **6**. It is noteworthy that in the case of the pure sodium phase the positions observed for sites M1 and M3 are very close to those found for the Cs<sup>+</sup>-exchanged phases in compounds **2**, **3**, **5**, and **6**. In other words, the cation and water sites in the pure sodium phase undergo only a minimal change on Cs exchange in their positions unlike the pure K phase where a large change occurs. As a consequence, the sodium phase is energetically more favorable for Cs uptake than the K-phase. In fact, this result is in good agreement with the ion exchange data<sup>25</sup> which show higher selectivity of Cs<sup>+</sup> by the sodium phase than for the K phase.

On the basis of ion exchange results and the bond distance data, it is clear that the preferred site for Cs<sup>+</sup> is M2, the site within the smaller cavity. However, the large Cs<sup>+</sup> cannot diffuse down the smaller channels because of the protrusion of oxygen atoms into the channels. Therefore, the large cations must enter the lattice through the 20-membered channel opening and diffuse into the smaller cavity. Since there are two large openings from the large channels to the small, a free flow of ions is possible. Neither in the large or small cavities are the bond distances to Na<sup>+</sup> favorable accounting for its ready displacement by larger ions. It may also account for the reason that we were not able to prepare the sodium phase directly.

The potassium trisilicate compound K<sub>2</sub>ZrSi<sub>3</sub>O<sub>9</sub>·H<sub>2</sub>O described here is analogous to umbite,<sup>26</sup> a mixed Zr/Ti silicate mineral with composition K<sub>2</sub>(Zr<sub>0.8</sub>Ti<sub>0.2</sub>)Si<sub>3</sub>O<sub>9</sub>·H<sub>2</sub>O. Umbite also crystallizes in the space group *P*2<sub>1</sub>2<sub>1</sub>2<sub>1</sub> with *a* = 10.208(2), *b* = 13.241(4), and *c* = 7.174(1) Å. As far as we are aware, the structure of this mineral is not characterized. Since the mineral belongs to the same space group and possess similar unit cell dimensions and molecular composition, it is likely to have the same structure as that of compound **1**. Interestingly, both umbite and the zirconium phases described in this paper convert to a hexagonal phase corresponding to the mineral wadeite at elevated temperatures. Therefore they may be considered as the precursors of the mineral wadeite, K<sub>2</sub>ZrSi<sub>3</sub>O<sub>9</sub>.<sup>27</sup> The structure<sup>28</sup> of wadeite, however, is entirely different from that of the title compound. In the title compound the trisilicate exists as a linear chain polymer as opposed to a condensed cyclic trisilicate in the mineral. The mineral crystallizes in the hexagonal space group

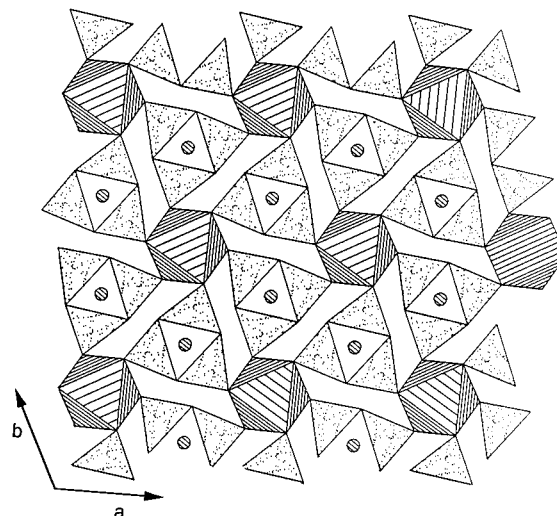


**Figure 6.** Structure of the mineral wadeite as viewed down the *c*-axis showing the K<sup>+</sup> ions sandwiched between the cyclic trisilicate groups.

*P*6<sub>3</sub>/*m* with *a* = *b* = 6.893 Å, *c* = 10.172 Å, *V* = 418.6 Å<sup>3</sup>, and *Z* = 2. The structure of the mineral down the *c*-axis is shown in Figure 6. The Zr atoms are located on the origin of the crystal lattice (site symmetry  $\bar{3}$ ) and they form layers in the *ab*-planes at *z* = 0 and 1/2. Within these metal layers, due to the  $\bar{3}$  symmetry, the Zr atoms occupy the corners of equilateral triangles. Therefore for a given Zr atom there are six surrounding triangles of Zr atoms in the *ab*-plane. The trisilicate exists as a nonplanar cyclic group. The centers of these cyclic trisilicate groups are located nearly at the centers of the Zr triangles, but they are shifted approximately halfway between successive Zr layers along the *c*-axis. The potassium ions, in fact, occupy exactly the centers of the Zr triangles in the *ab*-plane, and they are shifted slightly (~0.6 Å) on either side of the metal planes. Thus, in the structure, the potassium ions are sandwiched between the two adjacent cyclic trisilicate groups along the *c*-axis. Raveau et al.<sup>29</sup> have prepared a series of compounds A<sub>2</sub>BSi<sub>3</sub>O<sub>9</sub> (A = K, Rb; B = Ti, Sn) whose structures are isomorphous with that of the wadeite. These compounds were obtained in the temperature range 830–1000 °C.

It is most likely that the orthorhombic hydrated phases converted to the dehydrated hexagonal phase through a lattice transformation according to a matrix shown in (I). This matrix

$$\begin{bmatrix} 0 & 0 & 1 \\ 0 & 1/2 & -1/2 \\ 1 & 0 & 0 \end{bmatrix} \quad (\text{I})$$

converts the unit cell dimensions of K<sub>2</sub>ZrSi<sub>3</sub>O<sub>9</sub>·H<sub>2</sub>O to a lattice with *a* = 7.196 Å, *b* = 7.57 Å, *c* = 10.298 Å, and  $\gamma$  = 118.4°. It can be seen that the  $\gamma$  angle is very close to 120° and that the *a*- and *b*-dimensions thus obtained are very close to the *a* (and *b*) dimension of the wadeite phase (6.89 Å). The *c*-axis in the mineral and the matrix transformed lattice also compare well, taking into account that the transformed lattice dimensions correspond to the presence of a water molecule in the lattice. It should, however, be stressed that the matrix cannot be used to convert the atomic positions among these two phases because the trisilicate groups exist in two different forms in the hydrated and dehydrated phases.

The titanium compound K<sub>2</sub>TiSi<sub>3</sub>O<sub>9</sub>·H<sub>2</sub>O is isomorphous with compound **1** with very similar *b*- and *c*-dimensions but with a slightly smaller *a*-dimension. The important point, however,

(25) Bortun, A. I.; Bortun, L. N.; Clearfield, A. Paper in preparation.

(26) Henshaw, D. E. *Mineral. Mag.* **1955**, *30*, 585.

(27) JCPDS (No. 35-709).

(28) Bragg, L. *The Crystalline State*, 44, Cornell Univ. Press: Ithaca, NY, 1965.

(29) Choisnet, J.; Deschanvres et, A.; Raveau, B. *J. Solid State Chem.* **1973**, *7*, 408.

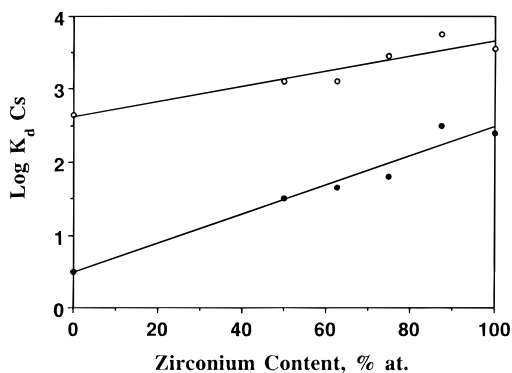


**Figure 7.** Plot of  $\log K_d^{\text{Cs}}$  for Cs uptake by the potassium Zr/Ti trisilicate as a function of Zr content determined for the exchanger in ground water simulant (○) and 5 M NaNO<sub>3</sub> + 1 M NaOH + 1 × 10<sup>-3</sup> M CsNO<sub>3</sub> solution (●). The affinity of the exchangers to Cs was expressed by the distribution coefficient ( $K_d$ , mL/g) which is given by  $K_d = (C_0 - C_0/C_i)V/m$ .  $C_0$  and  $C_i$  are the ion concentrations in the initial solution and in the solution after equilibrium with adsorbant, respectively.

is that unlike the Zr compound the Ti compound shows only very little preference for Cs<sup>+</sup> ions. Only about 10% of the K<sup>+</sup> ions in the structure can be replaced by Cs<sup>+</sup> ions. On substitution of Zr for Ti atom, the Cs uptake increases and it is directly proportional to the amounts of zirconium atom present in the compound. This property is graphically represented in Figure 7. The uptake of Cs by the Zr, Ti, and the mixed Zr/Ti

compounds in their potassium forms was studied by the batch technique at ambient temperature using a contact time of 5 days. The initial and final concentrations of the Cs<sup>+</sup> ions in the ground water (composition in ppm, Ca 100, Mg 10, Na 15, and Cs 5.95; volume to mass ratio  $V:m = 1000:1$  mL/g) and the model solutions (5 M NaNO<sub>3</sub> + 1 M NaOH + 1 × 10<sup>-3</sup> M CsNO<sub>3</sub>;  $V:m = 200:1$  mL/g) were measured using a Varian Spectra AA-300 atomic absorption spectrometer. A full description of the structure of the titanium compound along with the ion exchange properties of this series of compounds will be published in a subsequent paper.<sup>30</sup>

**Acknowledgment.** We acknowledge with thanks financial support of this study by the U.S. Department of Energy, Grant No. 198567-A-F1, through the Pacific Northwest National Laboratory under DOE's office of Science and Technology's Efficient Separation and Processing Crosscutting Program and by DOE's Basic Energy Sciences, Grant No. 43741-0001, with funds supplied by Environmental Management.

**Supporting Information Available:** Tables of atomic positions and thermal parameters for compounds 2–6 (Tables S1–S5), bond angles for all the structures (Table S6) and final Rietveld difference plots for compounds 2–6 (12 pages). Ordering information is given on any current masthead page.

IC970052Y

(30) Bortun, A. I.; Bortun, L. N.; Poojary, D. M.; Clearfield, A. *Chem. Mater.*, submitted for publication.